Testing for difference between two groups of functional neuroimaging experiments

Finn Årup Nielsen*†, Andrew C. N. Chen‡, Lars Kai Hansen†

July 5, 2004

Abstract

We describe a meta-analytic method that tests for the difference between two groups of functional neuroimaging experiments. We use kernel density estimation in three-dimensional brain space to convert points representing focal brain activations into a voxel-based representation. We find the maximum in the subtraction between two probability densities and compare its value against a resampling distribution obtained by permuting the labels of the two groups. The method is applied on data from thermal pain studies where "hot pain" and "cold pain" form the two groups.

1 Introduction

Human functional neuroimaging examines the relationship between cognitive functions and brain area with positron emission tomography (PET) or magnetic resonance imaging (MRI) brain scanners. Experiments typically investigates a specific brain function and determines its "activation" in the brain volume. This is usually done by scanning multiple subjects while they are under two different conditions (e.g., "activation" and "rest"). Statistical analysis of the scanning often employing the general linear model results in a statistical parametric image volume, that is summarized by the significant local maxima (Friston et al., 1995). These local maxima are presented in scientific articles by their 3-dimensional coordinate and, e.g., their z-score or p-value.

Before the statistical analysis the brain scans are spatially normalized to a standard brain atlas, — the so-called "Talairach atlas" (Talairach and Tournoux, 1988). This allows the 3-dimensional coordinates of the local maxima — the "Talairach coordinates" to be compared across studies.

If meta-analysis are to be performed then optimal we should use the statistical parametric image volume. Although there are beginning to appear neuroimaging databases that contain such data, e.g., the fMRI Data Center (Van Horn et al., 2001) and NeuroGenerator (Roland et al., 2001), the image volumes are typically not available and we have to resort to the Talairach coordinates.

The access to the Talairach coordinates is made easier when they are represented in a database. Two such databases exist: The BrainMap database

*Neurobiology Research Unit, Rigshospitalet, Copenhagen
†Informatics and Mathematical Modeling, Technical University of Denmark, Lyngby
‡Center of Sensory-Motor Interaction, Aalborg University, Aalborg

(Fox and Lancaster, 1994; Fox and Lancaster, 2002) and the Brede database (Nielsen, 2003), and a number of studies have modeled the distribution of the Talairach coordinates, e.g., (Fox et al., 1997; Nielsen and Hansen, 2002).

If the Talairach coordinates are restricted to a specific area their distribution may be approximated with a Gaussian distribution and inference can be made with parametric models (Fox et al., 1997) and, e.g., the Hotelling's T^2 can be employed to test the difference between two groups of coordinates (Christoff and Grabrieli, 2000). However, in many cases the distribution of the Talairach coordinates will have several spatial modes, and therefore it has been suggested to use Gaussian mixture models (Nielsen, 2001) or kernel density estimators (Nielsen and Hansen, 2002; Turkeltaub et al., 2002; Chein et al., 2002; Wager et al., 2003).

When the statistic analysis is performed it is usually in a mass-univariate setting where the number of statistical tests corresponds to the number of voxels in the volume. This results in a massive multiple comparison problem that is most often countered by employing random field theory for the statistical inference (Cao and Worsley, 2001). But permutation tests can also be used by constructing the null distribution for the maximum statistics, where the maximum is taken across all the voxel in the statistical parametric image (Holmes et al., 1996; Nichols and Holmes, 2001).

Below we will describe a meta-analytic method that uses permutation tests together with maximum statistics and kernel density estimation to give a statistical value for the difference between two groups of Talairach coordinates and thereby testing if two groups of functional neuroimaging experiments are different. We will use Talairach coordinates from hot and cold pain experiments. The pain modality is of special interest for our particular method since it typically causes a multimodal activation pattern where several district brain regions are involved: Thalamus, the somatosensory cortex, insula and anterior cingulate cortex (Ingvar, 1999).

2 Methods

A probability density volume is constructed from a local maximum l (in the following called "location") positioned in Talairach space at $\mathbf{x}_l$ by a 3-dimensional Gaussian kernel with isotropic variance (Nielsen and Hansen, 2002; Turkeltaub et al., 2002; Chein et al., 2002).

$$p(\mathbf{x}|l) = (2\pi\sigma^2)^{-3/2} \exp\left[-\frac{(\mathbf{x}-\mathbf{x}_l)^\mathsf{T}(\mathbf{x}-\mathbf{x}_l)}{2\sigma^2}\right]. \tag{1}$$

When we construct the probability density corresponding to a group of experiments $p(\mathbf{x}|g)$ we combine the contributions from all the individual locations associated with the group

$$p(\mathbf{x}|g) = \sum_{l\in g} p(\mathbf{x}|l)\, p(l|g), \tag{2}$$

where the prior is simply set to $p(l|g) = 1/|L_g|$, i.e., inversely proportionally to the number of locations in the g group. The continuous probability density is converted to a vector by sampling it in a regular grid

$$\mathbf{v}_g \equiv p(\mathbf{x}|g). \tag{3}$$

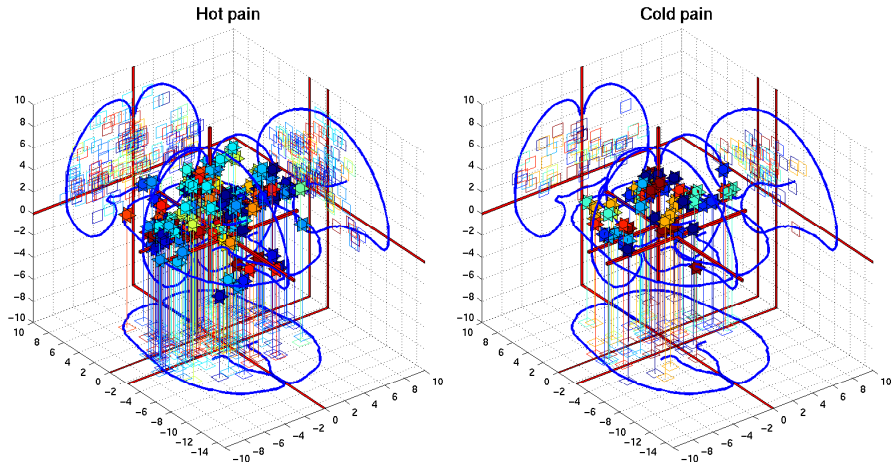

(a) Hot pain (b) Cold pain

Figure 1: Visualization of the Talairach coordinates from hot pain and cold pain studies in a corner cube environment (Rehm et al., 1998). The glyphs are colored according to the experiment they belong to and are projected onto the walls. The blue curves are the outline of the brain. The thick red lines are the axes of the Talairach atlas and the view point makes the upper left part of the back of the brain the closest point.

In the present application we use a coarse grid of $(8\text{mm})^3$ resulting in 7752 voxels. As a statistics for the difference between two volumes ($\mathbf{v}_1$ and $\mathbf{v}_2$) we simply use the subtraction performed separately for each voxel

$$\mathbf{t} = \mathbf{v}_1 - \mathbf{v}_2. \tag{4}$$

To counter the multiple comparison problem a null distribution use the maximum value across voxels

$$t = \max_i(t_i) \tag{5}$$

The null distribution of this maximum statistics is established by permutation: A distribution is build up by permuting the assignment of experiments to the two groups resulting in two new groups $\mathbf{v}_1^*$ and $\mathbf{v}_2^*$, that each comprises of the same number of experiments as the original two groups, thus the null distribution of the maximum statistics appear as

$$t^* = \max_i(v_{1,i}^* - v_{2,i}^*). \tag{6}$$

The permutation is randomized sufficiently many times to generate a "smooth" and stable distribution.

To demonstrate the method we invoke data from thermal pain studies, where the two groups are hot and cold pain. Such studies will typically employ a $45 - 50\,^\circ\text{C}$ or $0 - 5\,^\circ\text{C}$ stimulus to the subjects. The studies were added to the Brede database (Nielsen, 2003). Slight variations among the studies appear

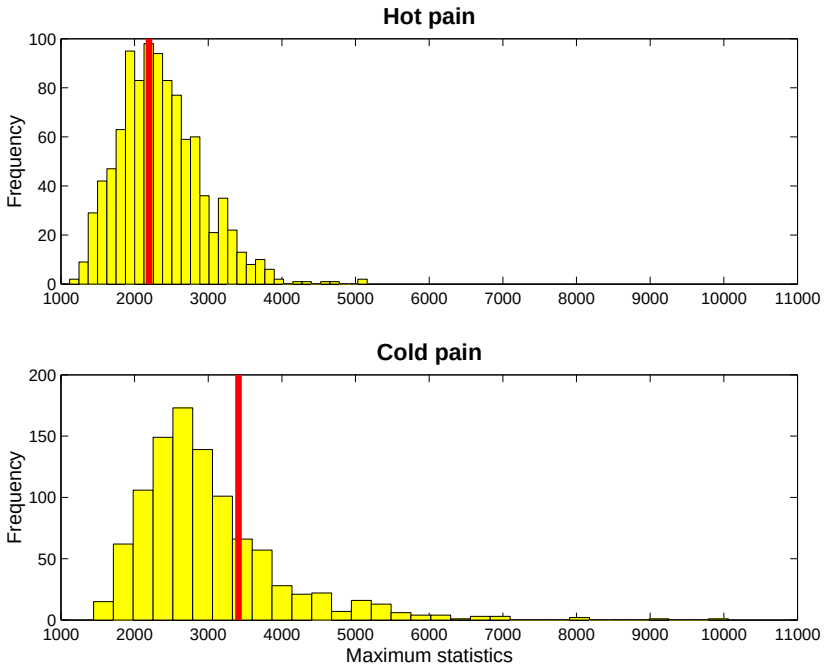

Figure 2: Empirical histogram of the maximum statistics after 1000 permutations. The red lines indicate the maxima for the hot and cold pain statistics t_{hot} and t_{cold}.

in the application of the Talairach atlases, and locations that conform to the so-called MNI space are adjusted before entry (Brett, 1999). All the locations from the pain experiments are shown in two panels in figure 1, where the color indicates the experiments the locations originate from. Table 1 lists all the included 24 hot and 8 cold pain experiments. Note that the pain stimulus is induced under varying contexts and some studies contributed with several experiments, e.g., a study by Faymonville *et al.* contributes with 6 experiments.

Both the statistics for hot and cold pain are considered, — simply by reversing the subtraction

$$t_{\text{hot}} = \max_i (v_{\text{hot},i} - v_{\text{cold},i}) \tag{7}$$

$$t_{\text{cold}} = \max_i (v_{\text{cold},i} - v_{\text{hot},i}) \tag{8}$$

Many of the operations performed in the method described above are implemented in the Brede Neuroinformatics Toolbox (Nielsen and Hansen, 2000).

3 Results and discussion

Figure 2 displays the empirical histogram of the null distribution of the maximum statistics t^*. The red lines indicate the maximum statistics of the comparisons of interest t_{hot} and t_{cold}. It indicates that our method does not find

1	WOEXT: 183 - Hot pain	(Tracey et al., 2000)
2	WOEXT: 186 - Attended heat pain on right hand	(Brooks et al., 2002)
3	WOEXT: 187 - Distracted heat pain on right hand	(Brooks et al., 2002)
4	WOEXT: 188 - Attended heat pain on left hand	(Brooks et al., 2002)
5	WOEXT: 189 - Distracted heat pain on left hand	(Brooks et al., 2002)
6	WOEXT: 217 - Hot pain in right hand	(Craig et al., 1996)
7	WOEXT: 225 - Hot pain on left hand (group 1)	(Becerra et al., 1999)
8	WOEXT: 227 - Hot pain on left hand (group 2)	(Becerra et al., 1999)
9	WOEXT: 230 - Painful heat on right fingers	(Gelnar et al., 1999)
10	WOEXT: 233 - Hot pain on right hand in rest, mental imagery and hypnosis	(Faymonville et al., 2000)
11	WOEXT: 234 - Hot pain on right hand in rest and mental imagery	(Faymonville et al., 2000)
12	WOEXT: 235 - Hot pain on right hand during hypnosis	(Faymonville et al., 2000)
13	WOEXT: 237 - Interaction between hypnosis and hot pain on right hand	(Faymonville et al., 2000)
14	WOEXT: 238 - Correlated with pain ratings in hot pain on right hand in rest, mental imagery and hypnosis	(Faymonville et al., 2000)
15	WOEXT: 240 - Interaction between hypnosis and pain ratings in hot pain on right hand.	(Faymonville et al., 2000)
16	WOEXT: 245 - Heat pain on right arm	(Tölle et al., 1999)
17	WOEXT: 246 - Positive correlation with pain threshold	(Tölle et al., 1999)
18	WOEXT: 248 - Correlation with pain intensity	(Tölle et al., 1999)
19	WOEXT: 249 - Correlation with pain unpleasantness	(Tölle et al., 1999)
20	WOEXT: 298 - Early phase heat pain	(Casey et al., 2001)
21	WOEXT: 299 - Late phase heat pain	(Casey et al., 2001)
22	WOEXT: 312 - Heat pain on left hand	(Vogt et al., 1996)
23	WOEXT: 314 - Heat pain on left volar forearm	(Adler et al., 1996)
24	WOEXT: 319 - Heat pain on left arm	(Casey et al., 1996)
1	WOEXT: 182 - Cold pain	(Tracey et al., 2000)
2	WOEXT: 184 - Cold pain in left hand	(Petrovic et al., 2000)
3	WOEXT: 213 - Cold pain in right hand	(Craig et al., 1996)
4	WOEXT: 263 - Cold pain on right foot	(Frankenstein et al., 2001)
5	WOEXT: 264 - Cold pain on right foot masked by silent word reading	(Frankenstein et al., 2001)
6	WOEXT: 265 - Silent word reading while cold pain on right foot	(Frankenstein et al., 2001)
7	WOEXT: 266 - Cold pain versus cold pain with silent word reading	(Frankenstein et al., 2001)
8	WOEXT: 320 - Cold pain on left arm	(Casey et al., 1996)

Table 1: List of included hot and cold pain experiments

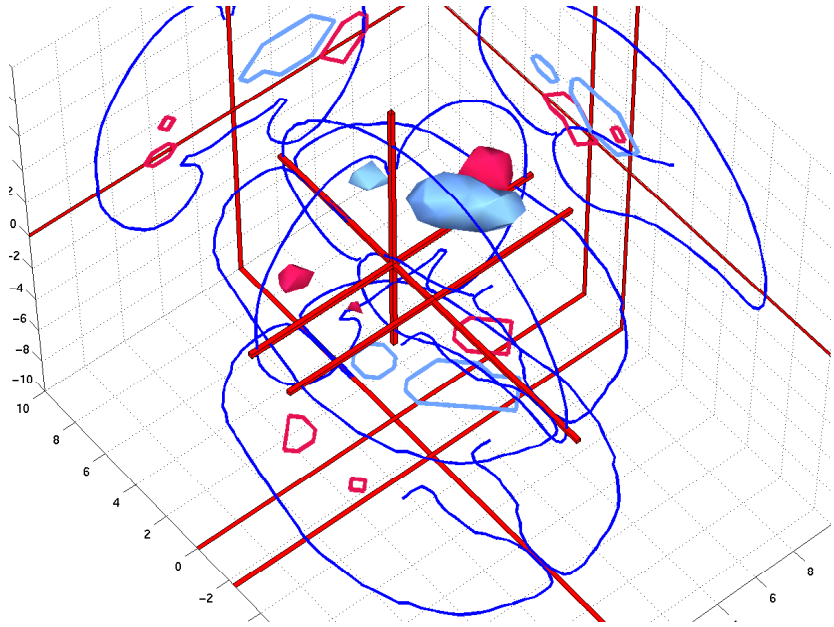

Figure 3: Results from the permutation test in a corner cube environment. Red isosurfaces are for hot pain and light blue isosurface is for cold pain.

any larger differences between hot and cold pain: The statistics of both hot and cold pain is found in the middle of the null distributions.

Figure 3 shows the result in a corner cube environment. Isosurfaces with a very liberal threshold are shown in the subtraction image for hot $\mathbf{t}_{\text{hot}}$ and cold pain $\mathbf{t}_{\text{cold}}$. The right hemisphere is the most is where any change first occure.

We have previously proposed a method that uses a database of experiments to generate a null distribution of the correlation coefficient between two volumes (Nielsen, 2004; Nielsen and Hansen, 2004). That method requires a database of dissimilar experiments to build up a null hypothesis, e.g., a pain experiment is compared with a memory or language experiment. The method we present in this contribution does not need this extra data, but relies only on data from the two groups that are being compared. Furthermore, our previous method is a global method performing an omnibus test for the entire volume, while our new method allows us to make inference on the voxel-level. Our presented method does, however, requires that there are sufficient experiments in each group for the reason of statistical power.

4 Acknowledgment

Jørgen Cold is acknowledgment for collection of the data. Finn Årup Nielsen is supported by the Villum Kann Rasmussen Foundation.

References

Adler, L. J., Gyulai, F. E., Diehl, D. J., Mintun, M. A., Winter, P. M., and Firestone, L. L. (1996). Regional brain activity changes associated with fentanyl analgesia elucidated by positron emission tomography. *Anesthesia & Analgesia*, 84(1):120–126.

Becerra, L. R., Breiter, H. C., Stojanovic, M., Fishman, S., Edwards, A., Comite, A. R., Gonzalez, R. G., and Borsook, D. (1999). Human brain activation under controlled thermal stimulation and habituation to noxious heat: An fMRI study. *Magnetic Resonance in Medicine*, 41(5):1044–1057.

Brett, M. (1999). The MNI brain and the Talairach atlas. http://www.mrc-cbu.cam.ac.uk/Imaging/mnispace.html. Accessed 2003 March 17.

Brooks, J. C. W., Nurmikko, T. J., Bimson, W. E., Singh, K. D., and Roberts, N. (2002). fMRI of thermal pain: effects of stimulus laterality and attention. *NeuroImage*, 15(2):293–301.

Cao, J. and Worsley, K. J. (2001). Applications of random fields in human brain mapping. In Moore, M., editor, *Spatial Statistics: Methodological Aspects and Applications*, volume 159 of *Lecture notes in Statistics*, chapter 8, pages 170–182. Springer, New York.

Casey, K. L., Minoshima, S., Morrow, T. J., and Koeppe, R. A. (1996). Comparison of human cerebral activation patterns during cutaneous warmth, heat pain, and deep cold pain. *Journal of Neurophysiology*, 76(1):571–581.

Casey, K. L., Morrow, T. J., Lorenz, J., and Minoshima, S. (2001). Temporal and spatial dynamics of human forebrain activity during heat pain: analysis by positron emission tomography. *Journal of Neurophysiology*, 85(2):951–959.

Chein, J. M., Fissell, K., Jacobs, S., and Fiez, J. A. (2002). Functional heterogeneity within Broca's area during verbal working memory. *Physiology & Behavior*, 77(4-5):635–639.

Christoff, K. and Grabrieli, J. D. E. (2000). The frontopolar cortex and human cognition: Evidence for a rostrocaudal hierarchical organization within the human prefrontal cortex. *Psychobiology*, 28(2):168–186.

Craig, A. D., Reiman, E. M., Evans, A., and Bushnell, M. C. (1996). Functional imaging of an illusion of pain. *Nature*, 384(6606):258–260.

Faymonville, M. E., Laureys, S., Degueldre, C., Del Fiore, G., Luxen, A., Franck, G., Lamy, M., and Maquet, P. (2000). Neural mechanisms of antinociceptive effects of hypnosis. *Anesthesiology*, 92(5):1257–1267.

Fox, P. T. and Lancaster, J. L. (1994). Neuroscience on the net. *Science*, 266(5187):994–996.

Fox, P. T. and Lancaster, J. L. (2002). Mapping context and content: the BrainMap model. *Nature Reviews Neuroscience*, 3(4):319–321.

Fox, P. T., Lancaster, J. L., Parsons, L. M., Xiong, J.-H., and Zamarripa, F. (1997). Functional volumes modeling: Theory and preliminary assessment. *Human Brain Mapping*, 5(4):306–311.

Frankenstein, U. N., Richter, W., McIntyre, M. C., and Remy, F. (2001). Distraction modulates anterior cingulate gyrus activations during the cold pressor test. *NeuroImage*, 14(4):827–36.

Friston, K. J., Holmes, A. P., Worsley, K. J., Poline, J.-B., Frith, C. D., and Frackowiak, R. S. J. (1995). Statistical parametric maps in functional imaging: A general linear approach. *Human Brain Mapping*, 2:189–210.

Gelnar, P. A., Krauss, B. R., Sheehe, P. R., Szeverenyi, N. M., and Apkarian, A. V. (1999). A comparative fMRI study of cortical representations for thermal painful, vibrotactile, and motor performance tasks. *NeuroImage*, 10(4):460–482.

Holmes, A. P., Blair, R. C., Watson, J. D. G., and Ford, I. (1996). Nonparametric analysis of statistic images from functional mapping experiments. *Journal of Cerebral Blood Flow and Metabolism*, 16(1):7–22.

Ingvar, M. (1999). Pain and functional imaging. *Philosophical Transactions of the Royal Society of London. Series B, Biological Sciences*, 354(1387):1347–1358.

Nichols, T. E. and Holmes, A. P. (2001). Nonparametric permutation tests for PET functional neuroimaging experiments: A primer with examples. *Human Brain Mapping*, 15(1):1–25.

Nielsen, F. Å. (2001). *Neuroinformatics in Functional Neuroimaging*. PhD thesis, Informatics and Mathematical Modelling, Technical University of Denmark, Lyngby, Denmark.

Nielsen, F. Å. (2003). The Brede database: a small database for functional neuroimaging. *NeuroImage*, 19(2). Presented at the 9th International Conference on Functional Mapping of the Human Brain, June 19–22, 2003, New York, NY. Available on CD-Rom.

Nielsen, F. Å. (2004). Assessing the reproducibility in sets of talairach coordinates. *NeuroImage*, 22. Presented at the 10th Annual Meeting of the Organization for Human Brain Mapping, June 14–17, 2004, Budapest, Hungary. Available on CD-ROM.

Nielsen, F. Å. and Hansen, L. K. (2000). Experiences with Matlab and VRML in functional neuroimaging visualizations. In Klasky, S. and Thorpe, S., editors, *VDE2000 - Visualization Development Environments, Workshop Proceedings, Princeton, New Jersey, USA, April 27–28, 2000*, pages 76–81, Princeton, New Jersey. Princeton Plasma Physics Laboratory.

Nielsen, F. Å. and Hansen, L. K. (2002). Modeling of activation data in the BrainMap^{TM} database: Detection of outliers. *Human Brain Mapping*, 15(3):146–156.

Nielsen, F. Å. and Hansen, L. K. (2004). Finding related functional neuroimaging volumes. *Artificial Intelligence in Medicine*, 30(2):141–151.

Petrovic, P., Petersson, K. M., Ghatan, P. H., Stone-Elander, S., and Ingvar, M. (2000). Pain-related cerebral activation is altered by a distracting cognitive task. *Pain*, 85(1-2):19–30.

Rehm, K., Lakshminarayan, K., Frutiger, S. A., Schaper, K. A., Sumners, D. L., Strother, S. C., Anderson, J. R., and Rottenberg, D. A. (1998). A symbolic environment for visualizing activated foci in functional neuroimaging datasets. *Medical Image Analysis*, 2(3):215–226.

Roland, P., Svensson, G., Lindeberg, T., Risch, T., Baumann, P., Dehmel, A., Frederiksson, J., Halldorson, H., Forsberg, L., Young, J., and Zilles, K. (2001). A database generator for human brain imaging. *Trends in Neuroscience*, 24(10):562–564.

Talairach, J. and Tournoux, P. (1988). *Co-planar Stereotaxic Atlas of the Human Brain*. Thieme Medical Publisher Inc, New York.

Tölle, T. R., Kaufmann, T., Siessmeier, T., Lautenbacher, S., Berthele, A., Munz, F., Zieglgansberger, W., Willoch, F., Schwaiger, M., Conrad, B., and Bartenstein, P. (1999). Region-specific encoding of sensory and affective components of pain in the human brain: a positron emission tomography correlation analysis. *Ann Neurol*, 45(1):40–7.

Tracey, I., Becerra, L., Chang, I., Breiter, H., Jenkins, L., Borsook, D., and Gonzalez, R. G. (2000). Noxious hot and cold stimulation produce common patterns of brain activation in humans: a functional magnetic resonance imaging study. *Neuroscience Letters*, 288(2):159–162.

Turkeltaub, P. E., Eden, G. F., Jones, K. M., and Zeffiro, T. A. (2002). Meta-analysis of the functional neuroanatomy of single-word reading: method and validation. *NeuroImage*, 16(3 part 1):765–780.

Van Horn, J. D., Grethe, J. S., Kostelec, P., Woodward, J. B., Aslam, J. A., Rus, D., Rockmore, D., and Gazzaniga, M. S. (2001). The functional magnetic resonance imaging data center (fMRIDC): the challenges and rewards of large-scale databasing of neuroimaging studies. *Philosophical Transactions of the Royal Society of London, Series B, Biological Sciences*, 356(1412):1323–1339.

Vogt, B. A., Derbyshire, S., and Jones, A. K. P. (1996). Pain processing in four regions of human cingulate cortex localized with co-registered PET and MR imaging. *European Journal of Neuroscience*, 8(7):1461–1473.

Wager, T. D., Phan, K. L., Liberzon, I., and Taylor, S. F. (2003). Valence, gender, and lateralization of functional brain anatomy in emotion: a meta-analysis of findings from neuroimaging. *NeuroImage*, 19(3):513–531.